BMC Plant Biology

RESEARCH

Open Access

A sexual/apomictic consensus linkage map of *Eragrostis curvula* at tetraploid level

Jimena Gallardo[1,2], Cristian Andrés Gallo[1], Martín Quevedo[1], José Carballo[1], Viviana Echenique[1,2*] and Diego Zappacosta[1,2*]

Abstract

Background Apomixis is an asexual reproduction process that allows plants to bypass meiosis and fertilization, resulting in clonal seeds that are genetically identical to the maternal genotype. *Eragrostis curvula* is a grass species used as model to disclose the mechanism associated to diplosporous apomixis. Previously, the first *E. curvula* linkage maps were developed using a F1 population derived from a cross between a sexual female parent (cv. OTA-S) and a facultative apomictic pollen donor (cv. Don Walter). Even though this work allows the identification a markers linked to apomixis in the male parent, the number of hybrids was not enough to produce a consensus map. Here, a new population is presented, increasing the number of genotyped hybrids to 107 which allows the construction of a consensus map and the development of KASP markers.

Results We constructed a consensus linkage map at the tetraploid level using a mapping population segregating for reproductive mode. Within this map, a region associated with apomeiosis (the *APO* locus) was identified using maternal and paternal SNP markers, along with three paternal markers that exhibited strong linkage with the trait. KASP markers were developed, one of which demonstrated 100% concordance with the cytoembryological phenotype of individuals in both the mapping population and other *E. curvula* genotypes. Through synteny analysis, the *APO* locus was mapped onto the *E. curvula* reference genome, and two genes that could be part of molecular pathways involved in apomeiosis were proposed.

Conclusions This study presents the first consensus genetic map and the development of KASP markers for phenotyping reproductive modes in *E. curvula*. This map enables the association of the apomixis-determining region with molecular markers from both parental genotypes, including the reference sexual tetraploid genotype of the species (OTA-S). The development and validation of co-dominant molecular KASP markers linked to the *APO* locus provide a crucial tool for future research and breeding.

Keywords Mapping, Weeping lovegrass, Apomixis, Apomeiosis

Introduction

Apomixis is an asexual reproduction process that allows plants to bypass meiosis and fertilization, resulting in clonal seeds that are genetically identical to the maternal genotype [55]. Apomixis is considered a polyphyletic trait and a striking example of convergent evolution, having independently evolved over one hundred times across more than half of the orders of flowering angiosperms (34 orders and 80 families) and is particularly prevalent in Asterales, Rosales and Poales [25]. Although

*Correspondence:
Viviana Echenique
echeniq@cerzos-conicet.gob.ar
Diego Zappacosta
dczappa@criba.edu.ar
[1] Centro de Recursos Naturales Renovables de La Zona Semiárida (CERZOS-CONICET, CCT Bahía Blanca), Bahía Blanca, Argentina
[2] Departamento de Agronomía, Universidad Nacional del Sur, Bahía Blanca, Argentina

apomixis occurs in 10% of the studied angiosperm species, it is absent in major crops such as maize, wheat and rice [27]. Apomixis in flowering plants requires three key elements: apomeiosis, parthenogenesis and the development of an endosperm to nourish the developing embryo. Endosperm formation in apomicts often occurs through a sexual process, however apomeiosis and parthenogenesis represent significant deviations from sexual reproduction [8]. There is a wide variety of apomictic mechanisms. In angiosperm, apospory is the most frequent type of apomictic development (357 species), followed by adventitious embryony (338 species) and diplospory (287 species) [27]. In adventitious embryogenesis, an apomictic embryo sac is not formed,instead, non-reduced embryos develop directly from a somatic cell of the nucellus or the ovule integuments. In apospory, the embryo sac originates directly through mitosis from a somatic cell, usually of the nucellus. In diplospory, the embryo sac arises from the megaspore mother cell, either through mitosis or as a result of meiotic failure.

The study of genetic factors involved in apomixis is complicated by the polyploid nature of most apomictic species, the limited availability of compatible sexual plants, and the difficulties in classifying progeny, particularly because components of apomixis can segregate. In citrus and mango, the inheritance of sporophytic apomixis is governed by a single dominant locus [7, 28]. In contrast, in some diplosporous apomictic species, the loci controlling the key apomixis components -apomeiosis, parthenogenesis and autonomous development of the endosperm- are independent of each other [19]. For instance, in *Erigeron* and *Taraxacum,* two independent loci controlling apomeiosis and parthenogenesis have been identified [34, 48]. In aposporous species, apomeiosis and parthenogenesis are determined by two different loci, as observed in *Hypericum* [42], *Poa* [5], and *Cenchrus* [17]. In *Hieracium*, three independent loci controlling apomeiosis, parthenogenesis, and autonomous endosperm development have been identified, *LOSS OF APOMEIOSIS* (*LOA*), *LOSS OF PARTHENOGENESIS* (*LOP*) and *Autonomous endosperm formation* (*AutE*), respectively [14, 35]. Based on segregation data, the genes controlling apomixis appear to be few in number, although, there is a lack of recombination in the chromosomal regions determining this trait, such as the apospory-specific genomic region (ASGR) in *Cenchrus ciliaris* [2].

The transfer of apomixis to crops would revolutionize agriculture as clonal F1 hybrid seeds with fixed heterosis can be indefinitely preserved and generated at low cost. This innovation would allow for greater investment in diverse germplasm and significantly shorten breeding cycles. Apomictic reproduction also has the potential to enhance seed set in genotypes that would otherwise be infertile or exhibit a high degree of heterosis (e.g., triploid and higher-ploidy hybrids). For these reasons, there is considerable interest in understanding the molecular mechanisms underlying apomixis for integration into breeding programs [25]. In recent decades, numerous studies have explored apomixis and its genetic control, focusing primarily on transferring apomictic reproduction to major economic crops. While several attempts have been made to introduce the trait into cultivated cereals, these efforts have not yet achieved complete success [30, 31].

Eragrostis curvula (Schrader) Nees, commonly known as weeping lovegrass, is a grass native to southern Africa. It was introduced to Argentina, USA, Australia and other countries nearly a century ago. Weeping lovegrass is an important crop in marginal areas with low rainfall and poor soils. It is commonly used as forage in semi-arid regions due to its ability to produce green forage until late autumn, its strong spring regrowth capacity, and its high adaptability. However, it has limitations, such as low palatability [23]. *Eragrostis curvula* includes genotypes with ploidy levels ranging from $2\times$ to $8x$ ($x=10$). Diploid genotypes reproduce sexually through cross-pollination, whereas polyploids reproduce via diplosporous apomixis. Although no sexual tetraploid genotypes have been identified in nature, an experimental genotype (cv. OTA-S) has been successfully developed [51].

Cytological evidence indicates that most polyploids of *E. curvula* are allopolyploids or segmental allopolyploids, as partial homology between subgenomes has been observed in some cases [39, 52]. This could explain the occurrence of apomixis in this species, as diplospory is considered a deregulation of the sexual process given that the formation of unreduced female gametophytes results from the interaction of distinct developmental programs between subgenomes [29]. Evidence suggests that apomictic reproduction is likely caused by genes with altered spatiotemporal expression patterns residing in duplicated genomic regions that share partial synteny with sexual genotypes or related species [22].

Diversity Array Technology (DArT-Seq) allows detailed and precise plant genetic characterization in a short time and at low cost, since it performs the sequencing of multiple samples simultaneously. In this way, tens to hundreds of thousands molecular markers can be identified from reduced genomic representations, using next-generation sequencing platforms [49]. DArT-Seq markers consist of SNPs and InDels and can provide a deep analysis of genetic diversity, whole-genome profiling and high-density mapping of complex traits. This technique has multiple advantages over other similar techniques such as GBS, since it generates more reliable data due to

the bioinformatics pipeline, the high-fidelity restriction enzymes used and to the intrinsic system of duplicated samples [41].

Cytoembryological phenotyping is a highly time-consuming task, and in weeping lovegrass, flow cytometry is not a viable option for phenotyping because the embryo:endosperm ploidy ratio is identical in seeds generated by both sexual or apomictic processes [33]. To address this limitation, we developed a molecular marker associated with apomixis based on previous transcriptomic studies, which identified a candidate gene present exclusively in apomictic genotypes. However, dominant markers have the disadvantage of producing false negatives due to problems in amplification. In contrast, codominant markers overcome this limitation and, when combined with KASP technology, offer additional advantages such as high-throughput genotyping, low cost and gel free genotyping [26]. The KASP genotyping assay employs a unique form of competitive allele-specific PCR along with a novel, homogeneous, fluorescence-based reporting system to identify and measure genetic variation at the nucleotide level, enabling the detection of single nucleotide polymorphisms (SNPs) or inserts and deletions (InDels) [26].

Recently, our group constructed the first linkage maps of *E. curvula* [58] using a mapping population derived from a cross between a sexual female parent (cv. OTA-S) and a facultative apomictic pollen donor (cv. Don Walter). This population was genotyped using SNPs markers obtained through GBS (genotyping by sequencing), as well as AFLP and SSR markers and separate linkage maps were made for each parental line. The total length of the linkage map for the sexual parent (cv. OTA-S) was 1,335 cM, with an average marker density of 0.82 markers/cM. For the apomictic parent (cv. Don Walter), the linkage map spanned 1,976.2 cM, with an average marker density of 1.02 markers/cM. The locus responsible for apomeiosis was mapped to linkage group 3 of Don Walter (now linkage group 9), with 66 other cosegregating markers. Among these, 4 SNPs were found to be 100% linked to the apomeiosis trait, defining a region of 10,492,321 bp in the cv. Victoria genome (*E. curvula* reference genome, [12]). Due to the small size of the mapping population (62 individuals), a consensus map could not be achieved. Therefore, it was not possible to link maternal and paternal markers and obtain a common linkage map for both parents. Neither could maternal markers be found for the linkage group where the apomeiosis locus is located.

In this study, we constructed a consensus linkage map at tetraploid level with a mapping population segregating for the reproductive mode in *E. curvula*. Within the map, a region associated with apomeiosis (*APO* locus) was identified using maternal and paternal SNP markers, as well as three paternal markers that showed a strong linkage with the trait. KASP markers were developed, one of which proved to be 100% concordant with the cytoembryological phenotype of indivuals of the mapping population and of other *E. curvula* genotypes. Through a synteny analysis, the *APO* locus was located in the reference genome of *E. curvula* and two genes that could be part of molecular pathways involved in apomeiosis were proposed. This information provides valuable insights into this complex trait and important tools for the crop.

Materials and methods

Plant material

To obtain the mapping population, the sexual *Eragrostis curvula* cv. OTA-S (United States Department of Agriculture, USDA, accession PI574506, 2n = 4*x* = 40) was crossed with the facultative apomictic *E. curvula* cv. Don Walter (Instituto Nacional de Tecnología Agropecuaria, INTA, 2n = 4*x* = 40) as pollen donor. Plants were grown in 5 L pots in the greenhouse under natural photoperiod and at a temperature of 25 ± 3 °C, in the city of Bahía Blanca, Argentina (38°43′0″S 62°16′0″W).

The mapping population was obtained in two stages. The first stage involved a population of 62 individuals [58], of which only 46 survived by the time of this study. Subsequently, additional crosses were performed between the same parental lines to increase the number of hybrids and enhance the robustness of the linkage map. This process is particularly laborious in weeping lovegrass since the small size of the spikelets makes not possible the emasculation, resulting in a large number of self-pollination seeds. Moreover, high seedling mortality was observed during the acclimatization. Finally, 265 new offprings were obtained, and their hybrid origin was evaluated using DArT-Seq markers. A principal component analysis (PCA) was performed with all the filtered SNPs markers to identify individuals sharing alleles from both parents, as non-hybrid individuals carry only maternal alleles.

DNA extraction

DNA was extracted according to the protocol described by Garbus et al. [24]. Briefly, 100 mg of young basal leaves tissue were cut into small portions and placed in 1.5 ml Eppendorf tubes containing 2 tungsten carbide beads (3 mm). The tubes were immersed into liquid nitrogen and the material was ground using a Tissuelyser II (Qiagen, USA). Then, 0.8 ml of extraction buffer (100 mM Tris HCl pH 8, 1.4 M NaCl, 20 mM EDTA pH 8, 2% (w/v) CTAB and 0.5 ml β-mercaptoethanol/100 ml of buffer) were added and then the samples were incubated for 30 min at 65 °C, inverting them regularly. Then, 0.4 ml of chloroform was added, left for 15 min at room temperature

and centrifuged at 12,000 RPM for 10 min. The supernatant (aqueous phase) was transferred to a new 1.5 ml Eppendorf tube and the DNA was precipitated with 0.64 ml of isopropanol. After this, the tube was centrifuged at 12,000 RPM for 1 min and the pellet was washed first with 70% ethanol and then with absolute ethanol. After drying the pellet in the laminar flow for 1 h, the DNA was resuspended in 50 µl of ultrapure water containing 20 µg/ml of RNase. DNA concentration and quality were analyzed with a DS-11 Series spectrophotometer (DeNovix®) and in 1.5% (w/v) agarose gels.

High-throughput genotyping using the DArT-Seq™ method

DNA samples from the mapping population individuals and six replicates of parental line were sent to the Agricultural Genetic Analysis Service of the International Maize and Wheat Improvement Center (SAGA-CIMMYT, Mexico) where they were processed (quantification, library preparation, sequencing and bioinformatics analysis). Libraries were prepared following the protocol described by Sansaloni et al. [41] and sequenced using an Illumina NovaSeq 6000 platform. The sequences generated from each sample were processed using specific pipelines developed for DArT-Seq. Initially, FASTQ files were filtered to remove low-quality sequences, with stricter selection criteria applied to the barcode region compared to the rest of the sequence. Identical sequences were then collapsed into'fastqcall'files, which were subsequently used in the secondary DArT-Seq pipeline for SNP calling (DArTsoft14).

SNP filtering

The SNPs markers obtained through DArT-Seq were filtered and selected based on the following criteria: first, markers with inconsistent alleles between replicates of each parental line were eliminated. Next, markers with homozygous alleles in both parental lines were removed. Finally, markers with more than 50% missing data in parental replicates or with more than 30% missing data in the population, were excluded. The filtered DArT-SNPs were then used to perform a principal component analysis (PCA) in TASSEL software to determine the hybrid origin of the 265 new offspring.

Phenotypic characterization

Hybrid offspring (46 individuals from the first mapping population and 61 from the new one) were phenotypically analyzed by cytoembryology through the observation of structures characteristic of apomictic or sexual processes. Panicles were collected at the onset of anthesis, a stage where all the stages of female development can be observed, from the archesporial cell to potential fertilization [33]. First, the spikelets were fixed in Farmer`s solution (25% glacial acetic acid, 75% absolute alcohol) and after 48 h they were transferred to 70% ethanol. The methyl salicylate clarification technique following the protocol described by Young et al. [56] with minor modifications was followed. Briefly, the fixed spikelets were incubated with shaking at room temperature in the following solutions: 95% ethanol (60 min),95% ethanol with 2% eosin (30 min), 100% ethanol (60 min); 75%/25% ethanol/methyl salicylate (60 min); 50%/50% ethanol/methyl salicylate (60 min), 25%/75% ethanol/methyl salicylate (60 min) and 100% methyl salicylate (24 h). Finally, the pistils were dissected from the spikelets under a stereo microscope (Leica S8 APO) and mounted with methyl salicylate for observation. The samples were observed under a microscope (Leica DM2500 LED, Germany) equipped with a differential interference contrast (DIC) system and a digital camera (Leica MC170 HD, Germany).

Linkage map construction

In addition to the criteria mentioned previously (see SNP filtering section), heterozygous markers present in only one parental line and exhibiting a segregation ratio of 1:1 (heterozygous:homozygous) in the offsprings were classified as single dose allele (SDA) markers and used for map construction. The Chi-square test in JoinMap 4.1 was used to assess deviations from the expected genotype segregation ratios. Therefore, markers with a Chi-square value greater than 10.91 (for maternal and paternal markers) or greater than 15 (for biparental markers) were excluded from the analysis. Furthermore, heterozygous markers in both parental lines (biparental markers) were also used to link markers from each parent and construct the consensus map.

For map construction the traditional approach using single-dose markers, as has been done in other studies with allopolyploids [53] was used. The consensus genetic linkage map was constructed using JoinMap 4.1 software [47], employing the complete cross-sib population (CP) option. Clustering analysis was performed with a LOD (log odds) score threshold of 6 or higher. Within each linkage group (LG), the Maximum Likelihood (ML) mapping algorithm was applied using default settings.

Synteny analysis

The physical positions of the DArT-Seq markers were searched for homology using BLAST 2.12.0 [6] against the *E. curvula* reference genome corresponding to the diploid cv. Victoria [12] with an Evalue $< e^{-10}$ as a criterion. These positions were used to assign each LG to a chromosome. Additionally, since the reference genome

used is available as one haplotype, we tried to identify homeologous chromosomes at tetraploid level.

KASP primer design

To validate the obtained map, apomeiosis linked SNPs were selected, and competitive allele-specific PCR primers (KASP) were designed based on their sequence. The KASP method enables rapid phenotyping using fluorescence. The Primer3Plus program was used to design the primers, incorporating specific "tails" for the FAM and HEX alleles, corresponding to the paternal and maternal alleles, respectively.

The KASP marker amplifications were performed following the protocol described by He et al. [26] and conducted using a PHERAstar Plus device at the GENeTyC service laboratory (Bahía Blanca, Argentina). The reaction mixture (10 µl total volume) consisted of 50 ng DNA, 5 µl of Master mix (containing fluorophores, dNTPs, and Taq polymerase) and 0.14 µl Assay mix (containing two specific primers and one common primer). Amplification reactions were carried out as follows: 1 cycle of 15 min at 94 °C, 10 cycles of 20 s at 94 °C, 60 s at 61 °C and 60 s at 72 °C and 26 cycles of 20 s at 94 °C, 60 s at 55 °C and 60 s at 72 °C. Samples without DNA were used as controls.

To validate the KASP marker linked to apomeiosis, cytoembryologically phenotyped *E. curvula* genotypes from a collection available at CERZOS were evaluated by duplicated (Table 1).

Table 1 *Eragrostis curvula* genotypes used to validate a KASP marker linked to apomeiosis. USDA: United States Department of Agriculture, USA; INTA: Instituto Nacional de Tecnología Agropecuaria, Argentina

Genotype (Accession)	Origin	Ploidy	Reproductive mode
PI 208214	USDA	Diploid	Sexual
PI 299919 525	USDA	Diploid	Sexual
PI 299920 531	USDA	Diploid	Sexual
PI 299928 569	USDA	Diploid	Sexual
OTA-S PI 574506	USDA	Tetraploid	Sexual
Ermelo PI 232986	USDA	Tetraploid	Apomictic
Tanganyika PI 234217	USDA	Tetraploid	Apomictic
Renner PI 591633	USDA	Tetraploid	Apomictic
Don Walter	INTA	Tetraploid	Apomictic
Tanganyika	INTA	Tetraploid	Apomictic
Don Eduardo	INTA	Hexaploid	Apomictic
Don Pablo	INTA	Heptaploid	Apomictic
Don Juan	INTA	Octoploid	Apomictic

Results

Development of the mapping population and F1 phenotyping

A PCA analysis was conducted using markers (filtered SNPs) from all individuals derived from the cross between OTA-S x Don Walter to select hybrid offsprings. Figure 1 shows the PCA plot, with two principal components accounting for 60% of the total variance. Based on this analysis, 107 hybrid individuals were selected, comprising 46 individuals from the previous population and 61 new hybrids. These hybrids exhibit alleles from both parental lines (Fig. 1, orange circle), whereas non-hybrid display only maternal alleles (Fig. 1, yellow circle).

Apomeiosis inheritance

The phenotyping of the mapping population was performed by assessing the presence of meiosis or apomeiosis processes in each hybrid individual. This was carried out through cytoembryology, as shown in Fig. 2. The presence of a tetrad or degenerating megaspores provides evidence of meiosis and sexual reproduction (Fig. 2A). In contrast, apomictic plants exhibit a clearly elongated megaspore mother cell with no signs of meiosis (Fig. 2E). The sexual embryo sac displays a distinct nuclear arrangement compared to the apomictic embryo sac. In the sexual bi- or tetranucleated embryo sac, 2 or 4 nuclei are positioned at opposite poles, respectively (Fig. 2B and C). However, in the apomictic embryo sac, the nuclei are grouped at the micropylar pole during bi- or tetranucleated stages (Fig. 2F and G). Finally, mature sexual embryo sac contains 8 or more nuclei (due to antipodal proliferation, Fig. 2D) whereas the apomictic embryo sac only contains 4 nuclei (without antipodals, Fig. 2H).

The phenotypic analysis identified 48 apomictic and 59 sexual hybrids, yielding a proportion close to 1:1 ($\chi^2 = 0.56$, df = 1). Although the apomictic:sexual hybrids ratio in the new mapping population differed slightly from that of the previous population, both ratios statistically corresponds to a 1:1 ratio.

Apomeiosis frequency in apomictic hybrids

Figure 3 shows the distribution of apomictic hybrids based on their reproductive mode. Interestingly, the proportion of apomictic processes among individuals in the mapping population was highly variable, ranging from 3 to 97% of apomictic pistils. This indicates that apomixis in *E. curvula* is a trait with highly variable expressivity, as previously reported [40, 57, 58].

SNPs filtering

The DArT-Seq pipeline generated a total of 120,349 SNPs (Suppl. Table 1). However, over 91% of the markers (110,208 SNPs) were discarded for being homozygous in both parents, rendering them unsuitable for linkage map construction. After additional filtering to remove markers with inconsistent alleles in parental replicates and

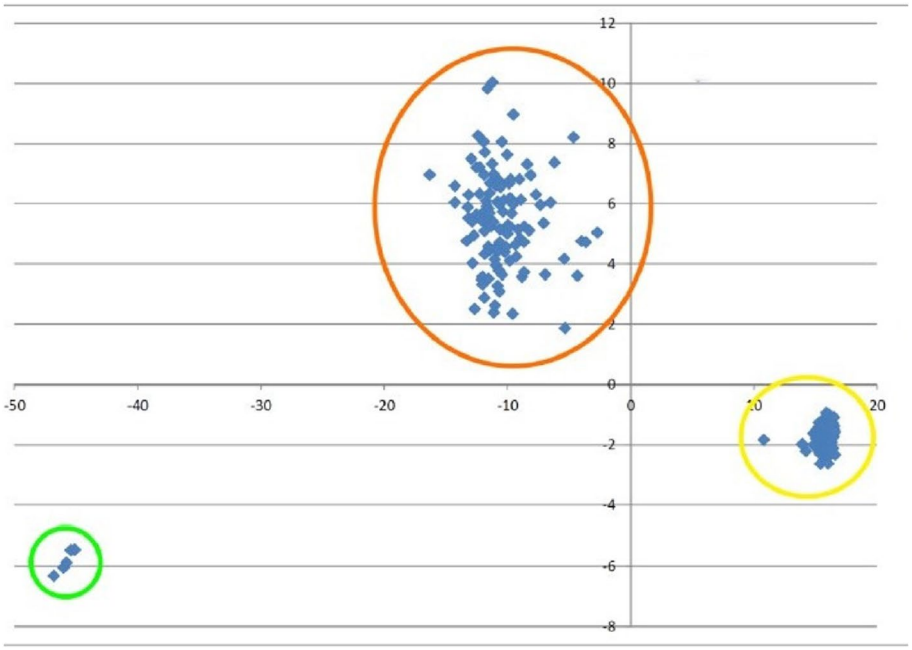

Fig. 1 Principal components plot of an *Eragrotis curvula* mapping population genotyped with DArT-Seq SNPs markers showing hybrid and non hybrid offspring. Yellow circle: cv. OTA-S samples and selfing individuals. Green circle: cv. Don Walter samples. Orange circle: hybrids from the OTA-S x Don Walter cross. X-axis represents the percentage of variance of principal component 1, and the Y-axis represents that of component 2

those with missing data, 2,522 markers remained, comprising 1,148 paternal, 993 maternal and 381 biparental markers.

Linkage map construction

The consensus linkage map was constructed with paternal, maternal and biparental markers with the JoinMap 4.1 software. Subsequently, since both parental genotypes are tetraploids, 20 LGs were formed using the Maximum Likelihood method with a LOD greater of 6 or higher. Figure 4 shows the consensus map in a marker density graph version, while Supplementary Fig. 1 shows the 20 LGs with the name and position of all markers.

The consensus map contained 1,132 markers, of which 587 were paternal, 514 were maternal and 31 were biparental markers. The total length of the map was 4,605 cM, with an average of 230 cM per LG. Table 2 shows the length and marker composition of each LG.

The apomeiosis locus (*APO* locus), defined as the region that contains three paternal SNP markers showing 100% co-segregation with apomeiosis, was mapped on LG9 of the consensus map (Fig. 5, for a detail Suppl. Figure 2).

Synteny analysis to identify homeologous groups

To identify homeologous groups in the consensus map, SNP markers sequences were mapped against the *E. curvula* reference genome corresponding to the sexual diploid cv. Victoria [12]. This strategy revealed that 86.6% of the markers were mapped to at least one of the assembled chromosomes. Synteny analysis demonstrated that markers belonging to the same LG tend to cluster on the same chromosome (Table 3). For instance, LG9, which contains the *APO* locus, is mainly enriched in Contig28 of the cv. Victoria reference genome. Figure 5 shows the region between the markers linked to the *APO* locus (100,477,277|F|0–6:C > T-6:C > T and 100,502,388|F|0–17:A > T-17:A > T) has a length of 11,322,729 bp (red circle). The *APO* locus, defined in the previous linkage map [58], is shown in the same Figure (Fig. 5, green box) as a region of 10,492,321 bp.

(See figure on next page.)

Fig. 2 Typical sexual (A-B-C-D) and apomictic (E–F-G-H) processes of *E. curvula* observed by DIC. A: Functional megaspore + degenerating megaspores, B: Sexual binucleated embryo sac, C: Sexual tetranucleated embryo sac, D: Mature sexual embryo sac with antipodal proliferation, E: Apomictic elongated megaspore mother cell, F: Apomictic binucleated embryo sac, G: Apomictic tetranucleated embryo sac, H: Apomictic mature embryo sac. deg: degenerant megaspores, FM: functional megaspore, EMMC: elongated megaspore mother cell, mn: micropylar nucleus, vac: vacuole, chn: chalazal nucleus, an: antipodal cells, ov: ovule, syn: synergid cells, pn: polar nucleus. Bar represents 50 µm

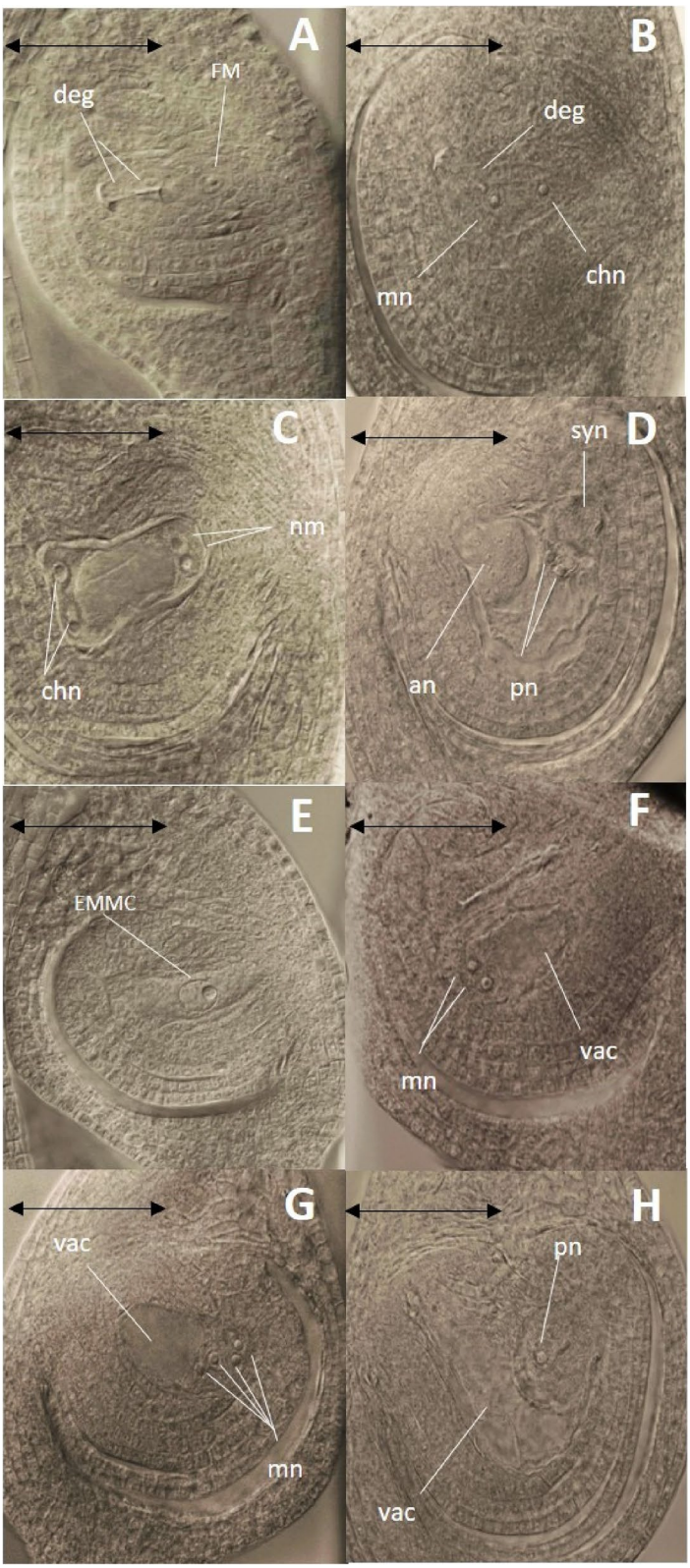

Fig. 2 (See legend on previous page.)

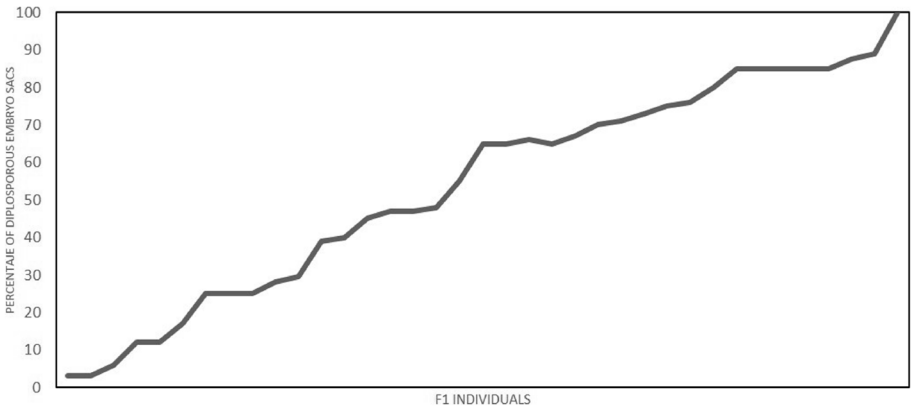

Fig. 3 Percentage of diplosporous processes in apomictic individuals of an *Eragrostis curvula* mapping population derived from the OTA-S x Don Walter cross

Analysis of the sequences of the SNPs linked to apomeiosis

For each of the three markers linked to apomeiosis, a sequence of 69 bp was obtained. These sequences were used to identify their counterparts in the reference genome (cv. Victoria). This analysis revealed that the three markers linked to the *APO* locus match gene sequences (two of them annotated), suggesting that these genes may be involved in apomeiosis.

The sequence obtained from the marker 100,477,277|F|0–6:C > T-6:C > T shows homology with an E3 ubiquitin ligase (Score: 988.63 (1095), E value: 0, Identity: 579/600 (96.5%), Gaps: 0/600 (0%)) (Suppl. Figure 3), while the sequence obtained from the marker 100,503,486|F|0–31:G > A-31:G > A shows homology with a D amino acid transaminase (Score: 1618.01 (1793), E value: 0, Identity: 946/979 (96.6%), Gaps: 0/979 (0%)) (Suppl. Figure 4). For the E3 ubiquitin ligase, two sequences (possibly alleles) were identified; both are present in the male parent (Don Walter), but only one is present in the female parent (OTA-S).

Validation of DArT-Seq SNPs markers associated with the *APO* locus

Five sets of KASP primers were designed (Table 4) and validated using DNA from the parental genotypes of the mapping population (OTA-S and Don Walter). Figure 6 (A, B, C, D and E) shows the spots corresponding to the presence of both alleles for each of the five sets of KASP primers. For the primers designed for the SNP 100502388|F|017:A > T-17:A > T, although replicates of both genotypes grouped correctly, the separation between parental replicas was unclear and positioned very close to the control (without DNA) compared to the results obtained from the other primers, indicating low amplification efficiency.

Based on their efficiency, the primers for SNP 100477277|F|0–6:C > T-6:C > T were selected and used for the evaluation of all the individuals of the mapping population. Figure 7 shows the grouping of the apomictic individuals with Don Walter samples and the sexual individuals with OTA-S samples, correlating closely with the cytoembryological phenotype. This validates the in silico data obtained and demonstrates the high performance of both the technique and the primers designed. To validate the KASP marker linked to apomixis, cytoembryologically phenotyped *E. curvula* genotypes from a collection available at CERZOS were used (Suppl. Figure 5).

Discussion

This study presents the first consensus genetic map and the development of KASP markers for phenotyping reproductive modes in *E. curvula*. The linkage map was generated using DArT-seq markers from a mapping population and includes 1,132 SNPs distributed across 20 linkage groups, covering 4,605 cM. This map enables the association of the apomixis-determining region with molecular markers from both parental genotypes, including the reference sexual tetraploid genotype of the species [50]. The development and validation of co-dominant molecular KASP markers linked to the *APO* locus provide a crucial tool for future research and breeding.

The new crosses performed between the tetraploid genotypes OTA-S and Don Walter resulted in 61 new hybrids that, combined with the 46 survivors of the previous mapping population [58], constituted a new mapping population of 107 hybrid individuals. Phenotyping of the offsprings identified 48 apomictic and 59 sexual individuals, a ratio close to 1:1 ($\chi^2 = 1.55$, df = 1), consistent with findings from previous studies [58]. This apomictic:sexual ratio aligns well with the model of a single gene or genome region governing the inheritance

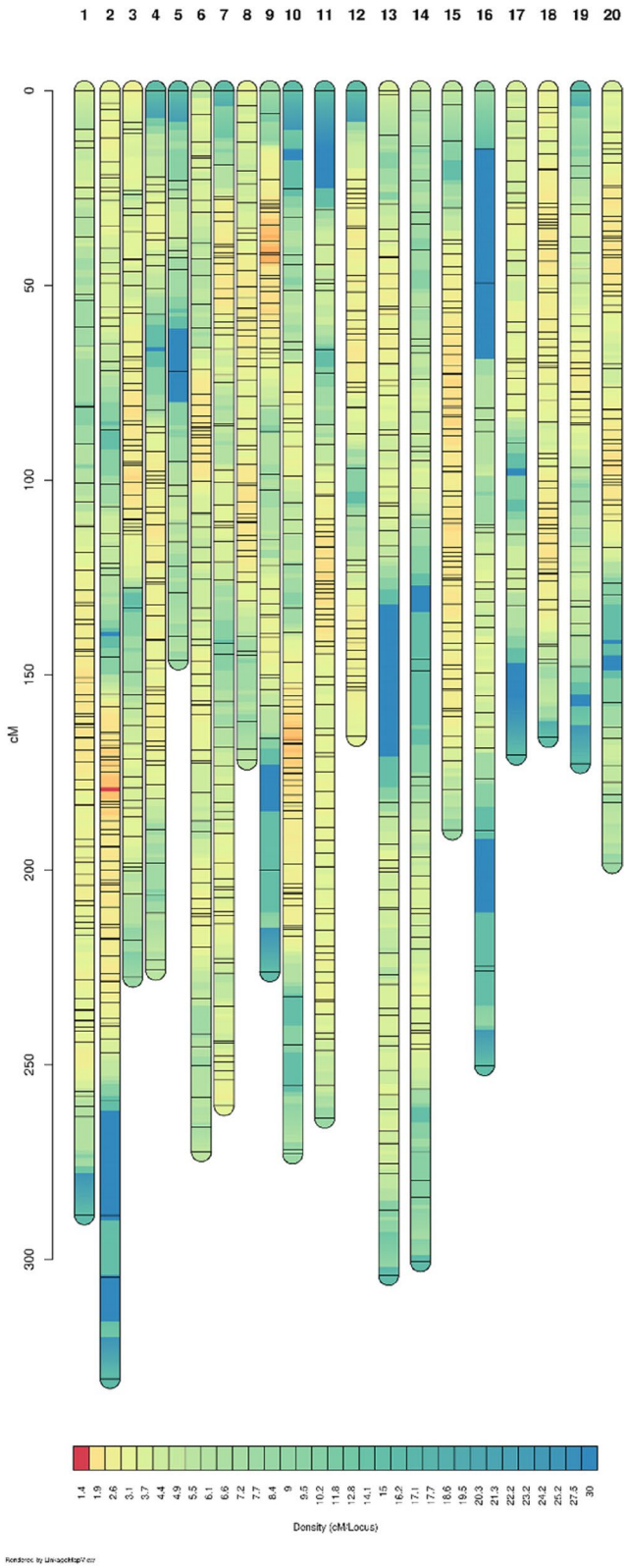

Fig. 4 *Eragrostis curvula* consensus linkage map obtained using a mapping population derived from the OTA-S x Don Walter cross. The heat map shows the marker density in each LG

Table 2 Summary of the 20 linkage groups (LG) of the *Eragrostis curvula* consensus linkage map derived from the cross OTA-S x Don Walter cross

Linkage Group	SNPs	Lenght (cM)	Paternal SNPs	Maternal SNPs	Biparental SNPs
LG1	78	288	50	27	1
LG2	82	330	50	30	2
LG3	64	227	19	44	1
LG4	58	225	26	31	1
LG5	19	146	8	9	2
LG6	73	272	49	23	1
LG7	65	260	32	31	2
LG8	55	171	23	30	2
LG9	54	226	31	20	3
LG10	68	272	60	7	1
LG11	71	263	32	38	1
LG12	49	165	36	12	1
LG13	61	304	17	41	3
LG14	48	300	13	34	1
LG15	71	189	31	38	2
LG16	30	250	5	22	3
LG17	34	170	29	4	1
LG18	60	166	32	27	1
LG19	34	172	12	21	1
LG20	57	198	31	25	1

of apomeiosis, with apomeiosis being dominant over sexuality. The new evidence, based on a large number of evaluated plants, further supports this model.

Our hypothesis is that sexuality represents the basic mode of reproduction, while apomixis is a derived mechanism that can suppress, but not entirely eliminate, sexuality. Additionally, other genes may control the penetrance and expressivity of apomixis, as the ratio of sexual and apomictic processes varies among apomictic individuals of the mapping population. Furthermore, the frequency of apomixis in the same plant can fluctuate across different blooming periods and under stress situations, suggesting the possibility of external regulation (outside the *APO* region) or involvement of epigenetic mechanisms [32, 40].

The increased size of the mapping population enabled the construction of a consensus map for *E. curvula*, a milestone not achieved in previous studies, alongside two separate maps for each parental line [58]. Wu et al. [54], recommend mapping populations of 75 or more individuals, suggesting that larger population sizes provide better mapping resolution [16]. Another improvement over the previous mapping effort was the construction of 20 LGs, instead of 40, corresponding to the haploid chromosome number of the parents and hybrids. Additionally, DArT-Seq markers were used for genotyping due to their greater reliability and precision [41, 49].

The new consensus map has a total length of 4,605 cM and 1,132 SNPs, being 514 maternal, 587 paternal and 31 biparental. The apomeiosis trait was located in LG9 of the consensus map with three linked SNP markers (100,477,277|F|0–6:C > T-6:C > T, 100,502,388|F|0–17:A > T-17:A > T and 100,503,486|F|0- 31:G > A-31:G > A). This situation aligns with reports in other models that describe a region with suppressed recombination controlling the trait, particularly within the Poaceae family, ensuring inheritance of all its components [3, 37]. In some species, such as *Cenchrus ciliaris*, this lack of recombination is evident when comparing markers associated with the apospory-specific genomic region (ASGR) to equivalent regions in maize and rice, finding in apomictic plants very small genetic distances in comparison to large physical distances in the reference sexual species [1].

The inheritance of apomixis and its components has been studied in other diplosporous species as well. In most cases, diplospory was dominant over sexuality and the locus determining diplospory and parthenogenesis are found unlinked, for example in *Erigeron annuus* [34], *Tripsacum dactyloides* [9], *Potentilla* spp. [21] and *Taraxacum officinale* [46]. The single dominant locus that

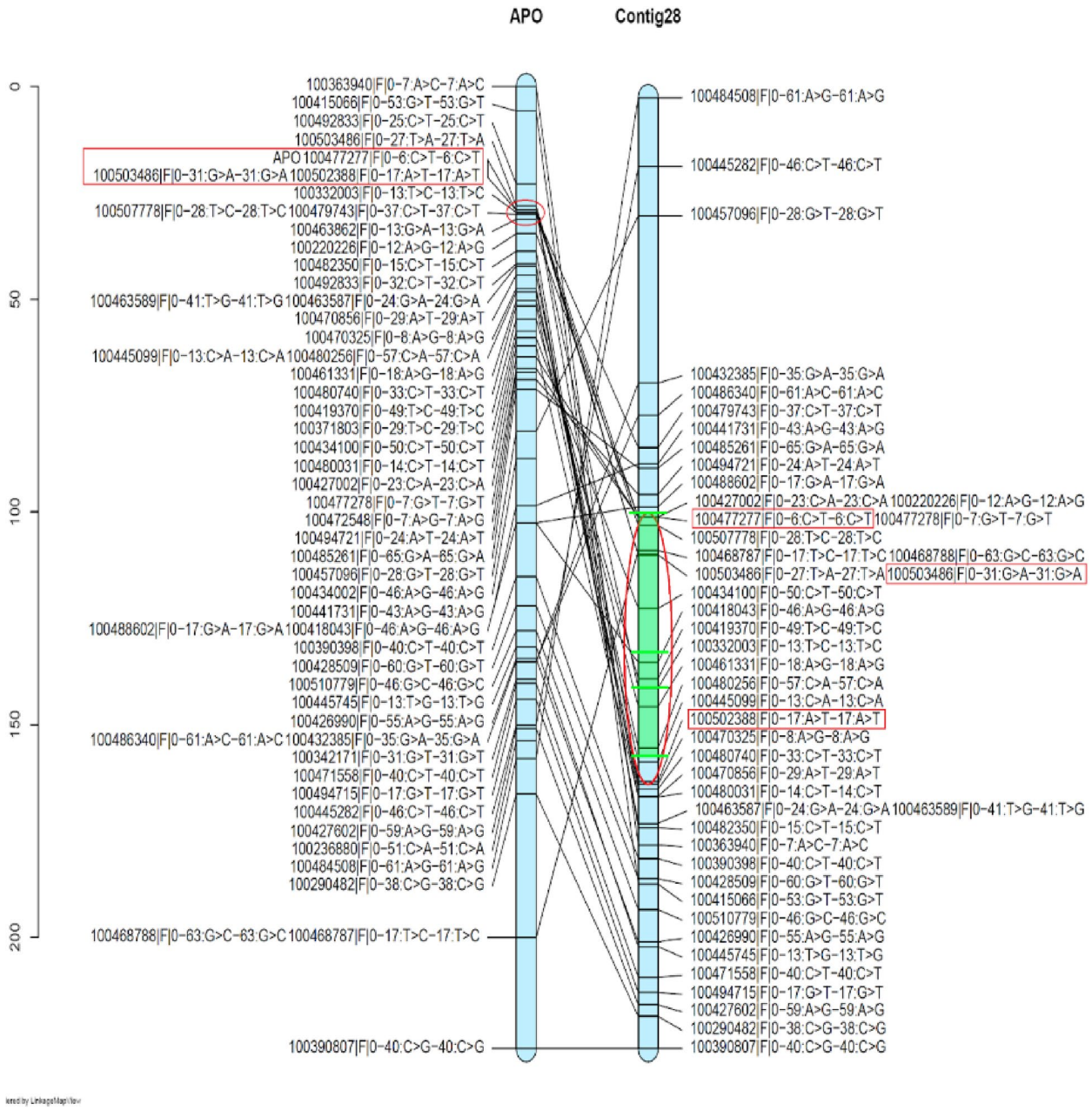

Fig. 5 Synteny between LG9 (*Eragrostis curvula* consensus map) and Contig28 of the reference genome (*E. curvula* cv. Victoria). Scale on the right represents cM. Red circle shows the *APO* locus region and the flanking markers linked on the consensus map. Green circle shows the *APO* region and the flanking markers previously mapped [58]

controls apomixis may not necessarily be a single master regulator but could involve several genetically linked genes, each controlling different aspects of the apomixis mechanism [9]. In *E. curvula*, it is still unknown whether apomixis expression is governed by a single region or if parthenogenesis and pseudogamy are determined by other co-segregating regions. The later hypothesis is more likely, based on other natural diplosporic models [19]. We are currently conducting studies to characterize and investigate the inheritance of parthenogenesis in our model species.

Synteny analysis using the high-quality reference genome assembly of *E. curvula* [12] allowed to associate all the consensus map LGs with the cv. Victoria chromosomes. This analysis also showed that the region flanked by the markers linked to the apomeiosis (*APO* locus)

Table 3 Synteny analysis between LGs of the consensus map obtained from an *Eragrostis curvula* mapping population segregating for the reproductive mode and the reference genome assembly of the species (*E. curvula* cv. Victoria). The last column shows the percentage of markers from each LG that match with the assembled contig

Linkage Group	cv. Victoria Genome	Contig length (bp)	Representation (%)
LG1	Contig38	57,060,119	75.64
LG2	Contig10	59,696,155	74.39
LG3	Contig3	45,712,337	76.56
LG4	Contig3	45,712,337	75.86
LG5	Contig8	28,838,055	68.42
LG6	Contig12	57,091,500	56.16
LG7	Contig50	26,185,977	49.23
LG8	Contig30	29,802,391	72.73
LG9	Contig28	42,455,315	81.82
LG10	Contig1	43,444,889	60.29
LG11	Contig8	28,838,055	76.06
LG12	Contig10	59,696,155	77.55
LG13	Contig12	57,091,500	57.38
LG14	Contig1	43,444,889	39.58
LG15	Contig25	23,821,556	80.28
LG16	Contig25	23,821,556	56.67
LG17	Contig12	57,091,500	52.94
LG18	Contig6	55,809,479	68.33
LG19	Contig8	28,838,055	82.35
LG20	Contig6	55,809,479	75.44

corresponds to a region of 11,322,729 bp in cv. Victoria reference genome assembly, Contig28. In the previous map the *APO* locus overlapped on the same region, but with a slightly shorter length, 10,492,321 [58]. Although this region is very large and contains hundreds of genes, similar results have been found in other model species. In *Pennisetum squamulatum*, the ASGR locus represents an extensive block of 50 Mbp that does not undergo recombination, ensuring the inheritance of all its components [1]. Given its large size, as estimated by physical mapping, a logical conclusion is that multiple genes may be required for apomixis, and an evolutionary mechanism to ensure their intact transmission would group them into a block. Such evolutionary patterns have precedents, as seen in self-incompatibility in *Brassica*, where several mechanisms may operate to reduce recombination and maintain linkage disequilibrium. These include divergence in allele sequence, chromosomal rearrangements, translocations, inversions and chromatine remodeling [11].

Although several reports describe candidate genes for apomixis in diverse model species, differentially expressed between sexual and apomictic genotypes or playing a functional role in apomictic development [4, 18, 20, 24, 43, 45, 53], little is known about the gene or genes that control regulatory programs or common pathways across different apomictic species or that trigger the trait. In the present study, the sequence of the SNPs linked to apomeiosis exhibited homology with proteins annotated in databases (NCBI, Swiss-Prot). Among these, one was an E3 ubiquitin ligase, a RING-type protein involved in ubiquitin-dependent protein degradation via the 26S proteasome. This pathway plays a critical role in regulating various cellular processes, including transcription, signal transduction, genetic recombination and cell cycle progression [15]. Differential expression of the ubiquitin pathway between apomictic and sexual genotypes has been documented in several studies, including research in *E. curvula* [13, 44], *Paspalum notatum* [10], *Hieracium praealtum* [36], *Hypericum perforatum* [22] and *Boechera* spp. [59]. The presence of two sequences, possibly alleles, of the E3 ubiquitin ligase in the apomictic genotype, compared to only one in the sexual genotype, suggests that this gene is a potential candidate involved in apomixis. Further studies will be conducted to elucidate its role in apomeiosis.

Another marker linked to apomeiosis exhibits homology with a D-amino acid transaminase, a key enzyme involved in the synthesis of non-essential amino acids and in aminoacid degradation. D-amino acid

Table 4 KASP primers designed for *Eragrostis curvula* SNPs validation. The first column indicates the primer name, second and third columns indicate the sequences of maternal (OTA-S) and paternal (Don Walter) alleles, respectively, fourth column the sequence of the common primer and the last column the specific nucleotide that belongs to sexual individuals and allows them to be distinguished from the apomictic allele

Primer	Maternal Allele Primer	Paternal Allele Primer	Common Primer	Sex
100,477,277|F|0–6:C > T-6:C > T	CATACCTCGTCGCTGCAGTT	CATACCTCGTCGCTGCAGTC	GACCACCCATCCGCCAGT	T
100477277 V2|F|0–6:C > T-6:C > T	CCAGTGACGTAACAATGGCA	CCAGTGATGTAACAATGGCG	GACCTCACATACCTCGTCG	A
100,502,388|F|0–17:A > T-17:A > T	TGAACCTGCAGTCTATTGATTTGA	TGAACCTGCAGTCTATTGATTTGT	TTTGGGACACGGGGTATTGG	A
100,503,486|F|0–31:G > A-31:G > A	TCTGGATCAGAATGCTGCGT	TCTGGATCAGAATGCTGCGA	AAGATCGACTCGCCGTTTCC	T
100503486 V2|F|0–31:G > A-31:G > A	GCCGTTTCCTCGCGAGAC	CCGTTTCCCCGCGAGAT	CATCTGGATCAGAATGCTGCG	C

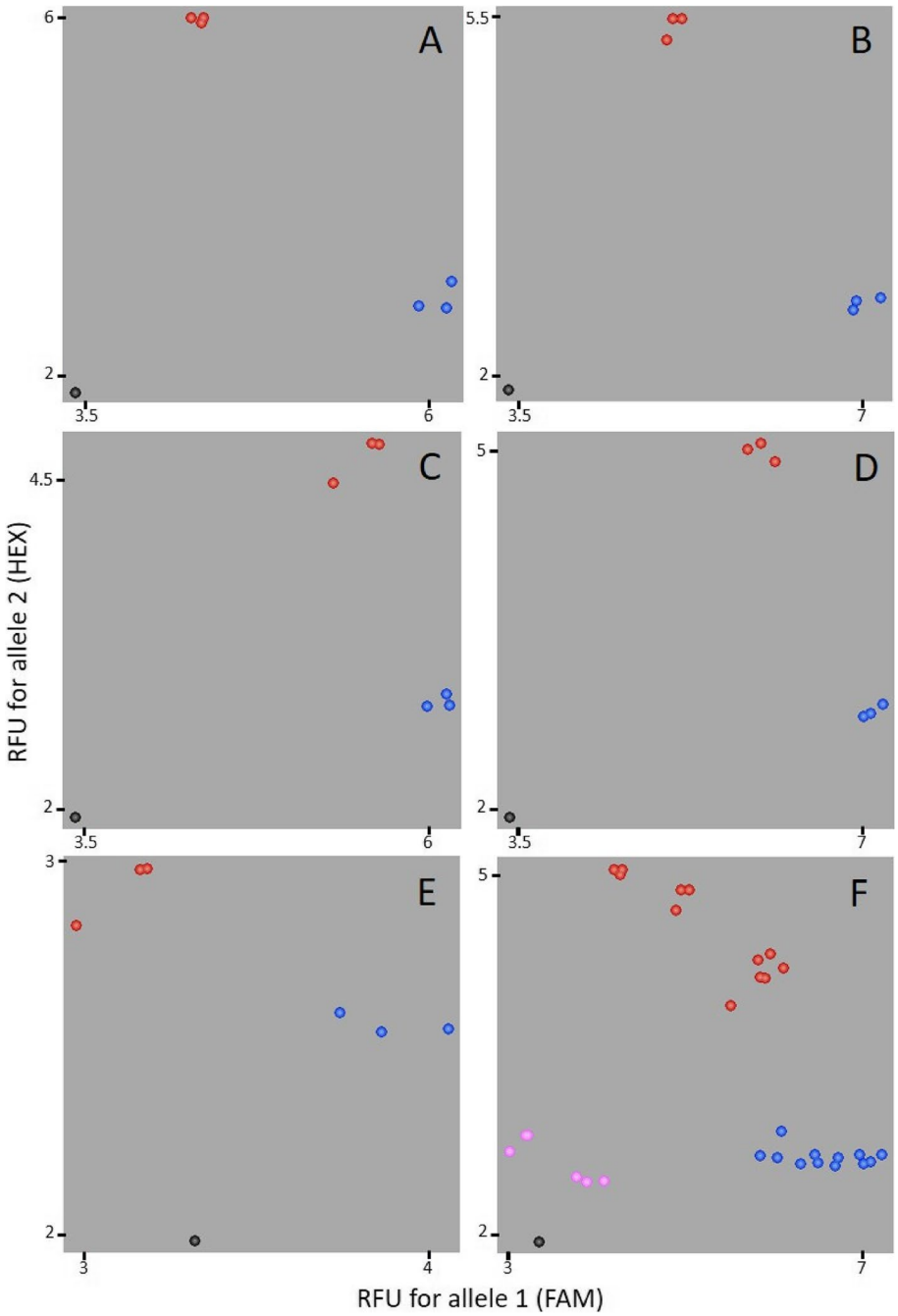

Fig. 6 DNA amplification of parental genotypes of the *E. curvula* mapping population using the sets of designed KASP primers (A: 100,477,277|F|0–6:C >T-6:C >T, B: 100477277 V2|F|0–6:C >T-6:C >T, C: 100,503,486|F|0–31:G > A-31:G > A, D: 100503486 V2|F|0–31:G > A-31:G > A, E: 100,502,388|F|0–17:A >T-17:A >T and F: all primers evaluated). Black dots correspond to control samples (without DNA), red dots represent Don Walter samples and blue dots indicated OTA-S samples. In graph F, pink dots correspond to samples amplified with primer 100,502,388|F|0–17:A >T-17:A >T. RFU: Relative FIruorescence Units

metabolism (DAT activity) has been crucial in supporting the metabolic functions required during the evolution of land plants, including processes such as pollen tube growth and the biosynthesis of vitamins and auxins [38]. This suggests that D-amino acid metabolism plays significant roles in plant biology, contributing not only to nitrogen metabolism but also to signaling pathways and plant development [38].

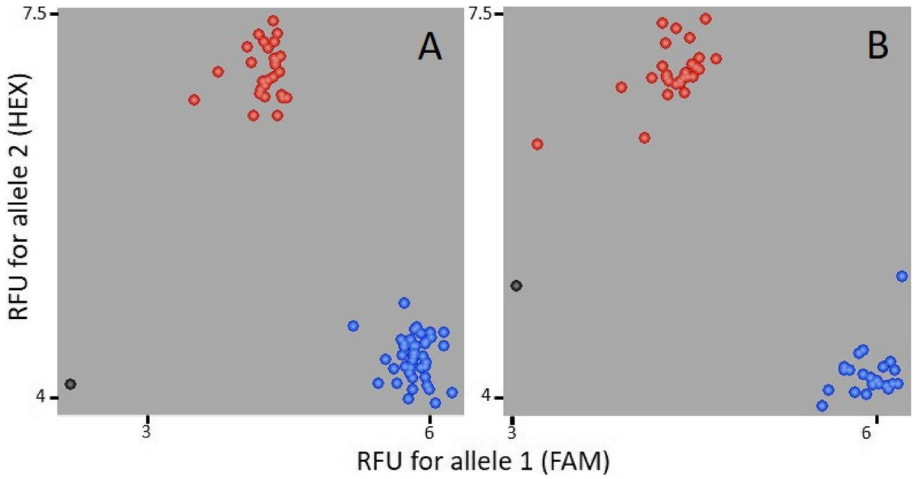

Fig. 7 Amplification of all individuals of the *Eragrostis curvula* mapping population with the set of KASP primers 100,477,277|F|0–6:C >T-6:C >T (A: new mapping population, B: previous mapping population). Black dots indicate the control sample, red dots represent Don Walter samples and the apomictic hybrids, and the blue dots correspond to OTA-S samples and the sexual hybrids. RFU: Relative FIruorescence Units

The development and validation of co-dominant molecular KASP markers linked to the *APO* locus in the mapping population and other *E. curvula* genotypes is an important tool developed in the present work. The use of these markers avoids the labor-intensive cytoembryologic phenotyping. Furthermore, their codominant nature is advantageous compared to dominant markers, as it reduces the risk of false negatives caused by amplification issues. Additionally, their methodological simplicity makes them an excellent tool for large scale phenotyping, both in research, such as mapping populations and in breeding programs for the identification and selection of apomictic individuals in segregating crosses.

A wide variety of apomictic mechanisms reflects the polyphyletic origin of the trait, suggesting the possibility of different determining genes across divergent species. Although significant progress has been achieved in identifying model species mutants with phenotypes resembling apomixis, gene discovery in non-model natural apomictic plants, particularly within a broad phylogenetic framework, offers a dual advantage. First, it complements synthetic approaches by enabling discovery and functional characterization of novel apomixis-related genes. Second, studying apomixis in species closely related to crops minimizes the risk of pleiotropic effects associated with large evolutionary distances, thereby improving the feasibility of introgression the trait into genotypes that may not be amenable to be transformed [25]. Consequently, it is of our best interest to continue identifying loci governing the components of apomixis in natural apomictic species to complement synthetic approaches and ensure the application of apomixis in agriculture.

Our model offers the advantage of having high-quality genome assemblies for a sexual diploid [12]. The most significant challenge in apomixis gene discovery lies in the lack of genomic resources for complex polyploid apomicts, which currently lack reference quality genomes. While promising results are beginning to emerge in a few species, the widespread application of apomixis in agriculture will require an expanded breeding toolkit, driven by the discovery of apomictic genes across multiple evolutionary lineages.

The results of this study, combined with future phenotyping of additional traits in the mapping population (e.g., lignin content and composition, drought resistance), will facilitate the implementation of marker-assisted and genomic selection in breeding programs for this orphan crop. The consensus map is a valuable tool for breeders to map important disease-resistance or other trait-associated genes.

Supplementary Information

The online version contains supplementary material available at https://doi.org/10.1186/s12870-025-06676-7.

Supplementary Material 1. Supplementary Figure 1. Linkage groups of the consensus linkage map generated using a mapping population derived from the OTA-S × Don Walter cross. Supplementary Figure 2. LG9 of the *Eragrostis curvula* linkage consensus map where the APO locus is located. The red box shows the APO locus, together with three linked SNPs markers. Scale on the right represents cM. Supplementary Figure 3. Blastn analysis of the sequence obtained from the marker 100477277|F|0-6:C>T-6:C>T that presents homology with an E3 ubiquitin ligase. Supplementary Figure 4. Blastn analysis of the sequence obtained from the marker 100503486|F|0-31:G>A-31:G>A that presents homology with a D-amino acid transaminase. Supplementary Figure 5: Amplification pattern of apomeiosis linked KASP marker in *E. curvula* genotypes from the CERZOS collection. Black dot indicate the control sample, red dots represent

apomictic genotypes, and the blue dots correspond to sexual genotypes. RFU: Relative FIruorescence Units.

Supplementary Material 2. Table 1. DArT-Seq file containing all markers obtained for the mapping population derived from the OTA-S × Don Walter cross.

Acknowledgements
This project has received funding from the European Union's Horizon 2020 Research and Innovation Program under the Marie Skłodowska-Curie Grant Agreement No 101007438 and Grant Agreement No 872417). This project also has received funding from CONICET (PIP-1220200101905CO), ANPCyT (PICT-2021-I-A-00576) and Universidad Nacional del Sur (PGI UNS 24/A261). The development and evaluation of the KASP markers were carried out in collaboration with, and at the facilities of, the GENeTyC laboratory (https://cerzos.conicet.gov.ar/index.php/servicios/laboratorios-de-servicios-stan/37-servicios-del-cerzos-genetyc).

Authors' contributions
DZ, and VE conceived and designed the study. DZ, and JG developed the mapping populations. MQ, and JG phenotyped mapping population. CAG, and JC performed the bioinformatic, genetic mapping and synteny analysis. All authors participated in manuscript elaboration. DZ and VE conducted and supervised the research and obtained funding.

Funding
This study has received funding from the European Union's Horizon 2020 Research and Innovation Program under the Marie Skłodowska-Curie Grant Agreement No 101007438 and Grant Agreement No 872417). This project also has received funding from CONICET (PIP-1220200101905CO), ANPCyT (PICT-2021-I-A-00576) and Universidad Nacional del Sur (PGI UNS 24/A261).

Data availability
All data generated or analysed during this study are included in this published article [and its supplementary information files].

Declarations

Ethics approval and consent to participate
Not applicable.

Consent for publication
Not applicable.

Competing interests
The authors declare no competing interests.

Received: 20 February 2025 Accepted: 5 May 2025
Published online: 17 May 2025

References

1. Akiyama Y, Conner J, Goel S, Morishige D, Mullet J, Hanna W, et al. High resolution physical mapping in *Pennisetum squamulatum* reveals extensive chromosomal heteromorphism of genomic region associated with apomixis. Plant Physiol. 2004;134:1733–41. https://doi.org/10.1104/pp.103.033969.
2. Akiyama Y, Hanna W, Ozias-Akins P. High-resolution physical mapping reveals that the apospory-specific genomic region (ASGR) in *Cenchrus ciliaris* is located on a heterochromatic and hemizygous region of a single chromosome. Theor Appl Genet. 2005;111:1042–51. https://doi.org/10.1007/s00122-005-0020-5.
3. Albertini E, Barcaccia G, Mazzucato A, Sharbel TF, Falcinelli M. Apomixis in the era of biotechnology. In: Pua E, Davey M, editors. Plant Developmental Biology - Biotechnological Perspectives. Berlin: Springer; 2010. p. 405–36. https://doi.org/10.1007/978-3-642-02301-9_20.
4. Albertini E, Marconi G, Reale L, Barcaccia G, Porceddu A, Ferranti F, Falcinelli M. SERK and APOSTART. Candidate genes for apomixis in *Poa pratensis*. Plant Physiol. 2005;138:2185–99. https://doi.org/10.1104/pp.105.062059.
5. Albertini E, Porceddu A, Ferranti F, Reale L, Barcaccia G, Romano B, Falcinelli M. Apospory and parthenogenesis may be uncoupled in *Poa pratensis*: a cytological investigation. Sex Plant Reprod. 2001;14:213–7. https://doi.org/10.1007/s00497-001-0116-2.
6. Altschul SF, Gish W, Miller W, Myers EW, Lipman DJ. Basic local alignment search tool. J Mol Biol. 1990;215:403–10. https://doi.org/10.1016/S0022-2836(05)80360-2.
7. Aron Y, Czosnek H, Gazit S. Polyembryony in mango (Mangifera indica L.) is controlled by a single dominant gene. HortScience. 1998;33:1241–2. https://doi.org/10.21273/hortsci.33.7.1241.
8. Bicknell R, Gaillard M, Catanach A, McGee R, Erasmuson S, Fulton B, Winefield C. Genetic mapping of the LOSS OF PARTHENOGENESIS locus in *Pilosella piloselloides* and the evolution of apomixis in the Lactuceae. Front Plant Sci. 2023;14:1239191. https://doi.org/10.3389/fpls.2023.1239191.
9. Blakey CA, Goldman SL, Dewald CL. Apomixis in *Tripsacum*: comparative mapping of a multigene phenomenon. Genome. 2001;44:222–30. https://doi.org/10.1139/g00-105.
10. Bocchini M, Galla G, Pupilli F, Bellucci M, Barcaccia G, Ortiz JPA, et al. The vesicle trafficking regulator PN_SCD1 is demethylated and overexpressed in florets of apomictic *Paspalum notatum* genotypes. Sci Rep-UK. 2018;8:3030. https://doi.org/10.1038/s41598-018-21220-4.
11. Boyes D, Nasrallah M, Vrebalov J, Nasrallah J. The self-incompatibility (S) haplotypes of *Brassica* contain highly divergent and rearranged sequences of ancient origin. Plant Cell. 1997;9:237–47. https://doi.org/10.1105/tpc.9.2.237.
12. Carballo J, Santos B, Zappacosta D, Garbus I, Selva JP, Gallo CA, et al. A high-quality genome of *Eragrostis curvula* grass provides insights into Poaceae evolution and supports new strategies to enhance forage quality. Sci Rep-UK. 2019;9:1–15. https://doi.org/10.1038/s41598-019-46610-0.
13. Carballo J, Zappacosta D, Marconi G, Gallardo J, Di Marsico M, Gallo CA, et al. Differential methylation patterns in apomictic vs. sexual genotypes of the diplosporous grass Eragrostis curvula. Plants. 2021;10:946. https://doi.org/10.3390/plants10050946.
14. Catanach AS, Erasmuson SK, Podivinsky E, Bicknell R. Deletion mapping of genetic regions associated with apomixis in *Hieracium*. P Natl A Sci USA. 2006;103:18650–5. https://doi.org/10.1073/pnas.060558810.
15. Chen L, Hellmann H. Plant E3 ligases: flexible enzymes in a sessile world. Mol Plant. 2013;6:1388–404. https://doi.org/10.1093/mp/sst005.
16. Collard BC, Jahufer MZ, Brouwer JB, Pang EC. An introduction to markers, quantitative trait loci (QTL) mapping and marker-assisted selection for crop improvement: the basic concepts. Euphytica. 2005;142:169–96. https://doi.org/10.1007/s10681-005-1681-5.
17. Conner JA, Gunawan G, Ozias-Akins P. Recombination within the apospory specific genomic region leads to the uncoupling of apomixis components in *Cenchrus ciliaris*. Planta. 2013;238:51–63. https://doi.org/10.1007/s00425-013-1873-5.
18. Conner JA, Mookkan M, Huo H, Chae K, Ozias-Akins P. A parthenogenesis gene of apomict origin elicits embryo formation from unfertilized eggs in a sexual plant. P Natl A Sci USA. 2015;112:11205–10. https://doi.org/10.1073/pnas.150585611.
19. Cornaro L, Banfi C, Cucinotta M, Colombo L, Van Dijk PJ. Asexual reproduction through seeds: the complex case of diplosporous apomixis. J Exp Bot. 2023;74:2462–78. https://doi.org/10.1093/jxb/erad054.
20. Corral JM, Vogel H, Aliyu OM, Hensel G, Thiel T, Kumlehn J, Sharbel TF. A conserved apomixis specific polymorphism is correlated with exclusive exonuclease expression in premeiotic ovules of apomictic *Boechera* species. Plant Physiol. 2013;163:1660–72. https://doi.org/10.1104/pp.113.222430.
21. Dobeš C, Milosevic A, Prohaska D, Scheffknecht S, Sharbel TF, Hülber K. Reproductive differentiation into sexual and apomictic polyploid cytotypes in *Potentilla puberula* (Potentilleae, Rosaceae). Ann Bot. 2013;112:1159–68. https://doi.org/10.1093/aob/mct167.
22. Galla G, Zenoni S, Avesani L, Altschmied L, Rizzo P, Sharbel TF, Barcaccia G. Pistil transcriptome analysis to disclose genes and gene products related to aposporous apomixis in *Hypericum perforatum* L. Front Plant Sci. 2017;8:79. https://doi.org/10.3389/fpls.2017.00079.

23. Gallardo J, Díaz M, Carballo J, Garayalde A, Echenique V. Phytolith content negatively affects forage quality of Eragrostis curvula (Schrad.) Nees. Agronomy. 2023;13:924. https://doi.org/10.3390/agronomy13030924 .
24. Garbus I, Romero JR, Selva JP, Pasten MC, Chinestra C, Carballo J, et al. De novo transcriptome sequencing and assembly from apomictic and sexual *Eragrostis curvula* genotypes. PLoS ONE. 2017;12:e0185595. https://doi.org/10.1371/journal.pone.0185595.
25. Goeckeritz CZ, Zheng X, Harkess A, Dresselhaus T. Widespread application of apomixis in agriculture requires further study of natural apomicts. iScience. 2024;27:110720. https://doi.org/10.1016/j.isci.2024.110720.
26. He C, Holme J, Anthony J. SNP genotyping: the KASP assay. Method Mol Biol. 2014;1145:75–86. https://doi.org/10.1007/978-1-4939-0446-4_7.
27. Hojsgaard D, Pullaiah T. Apomixis in angiosperms: mechanisms, occurrences, and biotechnology. Oxon, UK: CRC Press; 2023.
28. Kepiro JL, Roose ML. AFLP markers closely linked to a major gene essential for nucellar embryony (apomixis) in *Citrus maxima* × *Poncirus trifoliata*. Tree Genet Genomes. 2010;6:1–11. https://doi.org/10.1007/s11295-009-0223-z.
29. Koltunow AM, Grossniklaus U. Apomixis: a developmental perspective. Annu Rev Plant Biol. 2003;54:547–74. https://doi.org/10.1146/annurev.arplant.54.110901.160842.
30. Kumar S. Epigenetic control of apomixis: A new perspective of an old enigma. Adv Plants Agric Res. 2017;7:00243. https://doi.org/10.15406/apar.2017.07.00243.
31. Mahlandt A, Singh DK, Mercier R. Engineering apomixis in crops. Theor Appl Genet. 2023;136:131. https://doi.org/10.1007/s00122-023-04357-3.
32. Matzk F, Prodanovic S, Baumlein H, Schubert I. The inheritance of apomixis in *Poa pratensis* confirms a five loci model with differences in gene expressivity and penetrance. Plant Cell. 2005;17:13–24. https://doi.org/10.1105/tpc.104.027359.
33. Meier M, Zappacosta D, Selva JP, Pessino S, Echenique V. Evaluation of different methods for assessing the reproductive mode of weeping lovegrass plants, Eragrostis curvula (Schrad.) Nees. Aust J Bot. 2011;59:253–61. https://doi.org/10.1071/BT10267 .
34. Noyes RD, Rieseberg LH. Two independent loci control agamospermy (apomixis) in the triploid flowering plant *Erigeron annuus*. Genetics. 2000;155:379–90. https://doi.org/10.1093/genetics/155.1.379.
35. Ogawa D, Johnson SD, Henderson ST, Koltunow A. Genetic separation of autonomous endosperm formation (AutE) from the two other components of apomixis in *Hieracium*. Plant Reprod. 2013;26:113–23. https://doi.org/10.1007/s00497-013-0214-y.
36. Okada T, Hu Y, Tucker MR, Taylor JM, Johnson SD, Spriggs A, Tsuchiya T, Oelkers K, Rodrigues JC, Koltunow AM. Enlarging cells initiating apomixis in *Hieracium praealtum* transition to an embryo sac program prior to entering mitosis. Plant Physiol. 2013;163:216–31. https://doi.org/10.1104/pp.113.219485.
37. Ozias-Akins P, van Dijk PJ. Mendelian genetics of apomixis in plants. Annu Rev Genet. 2007;41:509–37. https://doi.org/10.1146/annurev.genet.40.110405.090511.
38. Porras-Dominguez J, Lothier J, Limami AM, Tcherkez G. D-amino acids metabolism reflects the evolutionary origin of higher plants and their adaptation to the environment. Plant Cell Environ. 2024;47:1503–12. https://doi.org/10.1111/pce.14826.
39. Poverene M. Contribución citogenética y quimiosistemática a la taxonomía del pasto llorón, *Eragrostis curvula* (Schrad.) Nees s. lat. Ph. D. Thesis. Bahía Blanca: Universidad Nacional del Sur; 1988.
40. Rodrigo JM, Zappacosta DC, Selva JP, Garbus I, Albertini E, Echenique V. Apomixis frequency under stress conditions in weeping lovegrass (*Eragrostis curvula*). PLoS ONE. 2017;12:e0175852. https://doi.org/10.1371/journal.pone.0175852.
41. Sansaloni C, Petroli C, Jaccoud D, Carling J, Detering F, Grattapaglia D, et al. Diversity Arrays Technology (DArT) and next-generation sequencing combined: genome-wide, high throughput, highly informative genotyping for molecular breeding of *Eucalyptus*. BMC Proc. 2011;5:54. https://doi.org/10.1186/1753-6561-5-S7-P54.
42. Schallau A, Arzenton F, Johnston AJ, Hähnel U, Koszegi D, Blattner FR, et al. Identification and genetic analysis of the APOSPORY locus in *Hypericum perforatum* L. Plant J. 2010;62:773–84. https://doi.org/10.1111/j.1365-313X.2010.04188.x.
43. Selva JP, Siena L, Rodrigo JM, Garbus I, Zappacosta D, Romero JR, et al. Temporal and spatial expression of genes involved in DNA methylation during reproductive development of sexual and apomictic *Eragrostis curvula*. Sci Rep-UK. 2017;7:1–11. https://doi.org/10.1038/s41598-017-14898-5.
44. Selva JP, Zappacosta D, Carballo J, Rodrigo JM, Bellido A, Gallo CA, et al. Genes modulating the increase in sexuality in the facultative diplosporous grass *Eragrostis curvula* under water stress conditions. Genes. 2020;11:969. https://doi.org/10.3390/genes11090969.
45. Siena LA, Ortiz JPA, Leblanc O, Pessino S. PnTgs1-like expression during reproductive development supports a role for RNA methyltransferases in the aposporous pathway. BMC Plant Biol. 2014;14:297. https://doi.org/10.1186/s12870-014-0297-0.
46. van Dijk PJ, Op den Camp RHM, Schauer SE. Genetic dissection of apomixis in dandelions identifies a dominant parthenogenesis locus and highlights the complexity of autonomous endosperm formation. Genes. 2020;11:961. https://doi.org/10.3390/genes11090961.
47. Van Ooijen JW. JoinMap R 4. Software for the calculation of genetic linkage map in experimental populations. Netherlands: Kyazma BV; 2006.
48. Vašut R, Vijverberg K, van Dijk PJ, de Jong H. Fluorescent *in situ* hybridization shows DIPLOSPOROUS located on one of the NOR chromosomes in apomictic dandelions (*Taraxacum*) in the absence of a large hemizygous chromosomal region. Genome. 2015;57:609–20. https://doi.org/10.1139/gen-2014-0143.
49. Vikram P, Franco J, Burgueño-Ferreira J, Li H, Sehgal D, Saint Pierre C, et al. Unlocking the genetic diversity of Creole wheats. Sci Rep-UK. 2016;6:23092. https://doi.org/10.1038/srep23092.
50. Voigt P. Registration of OTA-S weeping lovegrass germplasm (Reg. No. GP 8). Crop Sci. 1976;16:886. https://doi.org/10.2135/cropsci1976.0011183X001600060044x.
51. Voigt P, Bashaw E. Facultative apomixis in *Eragrostis curvula*. Crop Sci. 1976;16:803–5. https://doi.org/10.2135/cropsci1976.0011183X001600060017x.
52. Vorster T, Liebenberg H. Cytogenetic studies in the *Eragrostis curvula* complex. Bothalia. 1977;12:215–21. https://doi.org/10.4102/abc.v12i2.1399.
53. Worthington M, Heffelfinger C, Bernal D, Quintero C, Zapata YP, Perez JG, et al. A parthenogenesis gene candidate and evidence for segmental allopolyploidy in apomictic *Brachiaria decumbens*. Genetics. 2016;203:1117–32. https://doi.org/10.1534/genetics.116.190314.
54. Wu KK, Burnquist W, Sorrells ME, Tew TL, Moore PH, Tanksley SD. The detection and estimation of linkage in polyploids using single-dose restriction fragments. Theor Appl Genet. 1192;83:294–300. https://doi.org/10.1007/BF00224274.
55. Xiong J, Hu F, Ren J, Huang Y, Liu C, Wang K. Synthetic apomixis: the beginning of a new era. Curr Opin Biotech. 2023;79:102877. https://doi.org/10.1016/j.copbio.2022.102877.
56. Young BA, Sherwood RT, Bashaw EC. Cleared-pistil and thick-sectioning techniques for detecting aposporous apomixis in grasses. Can J Bot. 1979;57:1668–72. https://doi.org/10.1139/b79-204.
57. Zappacosta D, Ochogavía A, Rodrigo JM, Romero J, Meier M, Garbus I, et al. Increased apomixis expression concurrent with genetic and epigenetic variation in a newly synthesized *Eragrostis curvula* polyploid. Sci Rep-UK. 2014;4:4423. https://doi.org/10.1038/srep04423.
58. Zappacosta D, Gallardo J, Carballo J, Meier M, Rodrigo JM, Gallo CA, et al. A high-density linkage map of the forage grass *Eragrostis curvula* and localization of the diplospory locus. Front Plant Sci. 2019;10:918. https://doi.org/10.3389/fpls.2019.00918.
59. Zühl L, Volkert C, Ibberson D, Schmidt A. Differential activity of F-box genes and E3 ligases distinguishes sexual versus apomictic germline specification in *Boechera*. J Exp Bot. 2019;70:5643–57. https://doi.org/10.1093/jxb/erz323.

Publisher's Note